For published version see Proc. Mater. Res. Soc. 1267, DD04-07 (2010), doi: 10.1557/PROC-1267-DD04-07

NMR AND COMPUTATIONAL STUDIES OF $Ba_8Ga_{16}Sn_{30}$ CLATHRATES

Sergio Y. Rodriguez[1], Xiang Zheng[1,2] and Joseph H. Ross, Jr.[1,2]
[1]Department of Physics and Astronomy, Texas A&M University, College Station, TX 77843-4242, U.S.A.
[2]Material Science and Engineering Program, Texas A&M University, College Station, TX 77843, U.S.A.

ABSTRACT

We report a study of type-VIII and type-I $Ba_8Ga_{16}Sn_{30}$. NMR lineshape measurements identify a broad first-order satellite resonance. Simulations for the type-I structure based on first principles calculations provided an excellent fit to the data, with the best agreement provided by configurations with 4 Ga-Ga bonds. However calculations indicate that preferred configurations should completely avoid Ga-Ga contact, similar to results for $Ba_8X_{16}Ge_{30}$ materials. These results allow us to address local configurations within the random type-I alloy, as well as atomic displacements and bond-length distributions, which we compare to experiment.

INTRODUCTION

The search for new thermoelectric materials is very important for potential applications such as regeneration of wasted heat. In 1997 Slack proposed that a good thermoelectric material would be one that can act as a "*phonon glass electron crystal*" [1]. Due to their thermal and electric properties clathrates have been shown to be good candidates for possible thermoelectric device application. Si, Ge and Sn clathrates are isomorphic to the hydrate clathrates, and have frameworks that house guest atoms inside their cages, usually group 1 and 2 elements. Small amounts of transition metals can be substituted in the framework giving a drastic change in thermal and electric properties. The general formula for both the type-I and type-VIII structures is X_8E_{46}. In type I every unit cell contains two dodecahedral cages and six tetrakaidecahedra. Meanwhile for type VIII the unit cell is composed of eight identical distorted dodecahedra.

Besides their thermal properties other interesting features of the clathrates include superconductivity [2] and possible Rabi oscillators [3]. $Ba_8Ga_{16}Sn_{30}$ is an interesting material because besides the possibility for carrier tuning, it shows a structural dimorphism, crystallizing as type VIII (α phase) or type I (β phase), depending on the annealing conditions. Both types have been shown to have low thermal conductivity with a similar behavior to amorphous SiO_2, together with prominent rattling behavior [4-6]. Thus it is important to study the variations in thermal and electrical behavior for the two different types of structures. Here we report measurements for both structures with detailed calculations for type I.

EXPERIMENT

Two type-VIII and two type-I samples of nominal composition $Ba_8Ga_{16}Sn_{30}$ were prepared from the pure elements, mixed according to the desired composition, with an initial arc melting under argon. Type VIII was obtained by subsequent annealing at 500 ˚C, while type I was obtained by soaking at 900 ˚C for 50 hours, then slow cooling (80 hours) to 500 ˚C, similar to the procedure reported by Suekuni *et al*. [4]. X-ray diffraction (XRD) measurements were performed on a Bruker D8 X-ray Powder Diffractometer, with Rietveld refinement performed using

EXPGUI [7]. Wavelength dispersion spectroscopy (WDS) measurements were done in a Cameca SX50 equipped with 4 wavelength dispersive x-ray spectrometers. NMR experiments were performed at a field of 9 T using a pulse spectrometer described previously [8].

Table I: Site occupations from type-I and type-VIII Rietveld refinements.

Sample	Atom	6*c*	16*i*	24*k*	Sample	Atom	2*a*	8*c*	12*d*	24*g*
I A	Ga	2.01	5.81	8.15	VIII A	Ga	0.55	2.13	5.15	6.50
I A	Sn	3.25	9.58	16.93	VIII A	Sn	1.38	4.82	6.97	16.42
I B	Ga	2.42	5.57	7.93	VIII B	Ga	0.32	2.83	5.22	6.49
I B	Sn	3.26	10.77	15.77	VIII B	Sn	1.25	5.21	5.43	17.97

From XRD and WDS measurements it was found that all samples consist of a type VIII or type I major phase, with a small $Ba(Ga,Sn)_4$ minor phase as well as some remaining Sn and Ga flux. The $Ba(Ga,Sn)_4$ amount is such that only about 1% of Ga atoms occur in this phase, giving negligible contribution to NMR measurements. We found no evidence for coexistence of type I and type VIII clathrate structures in these samples. The refined Ga and Sn framework occupation values are summarized in Table I. In scans of our samples by WDS, the obtained composition assuming a completely full framework for type I is $Ba_{7.80}Ga_{16.15}Sn_{29.85}$, and for type VIII $Ba_{7.66}Ga_{16.28}Sn_{29.72}$. If we assume that the framework occupation is similar to the sum of the Ga and Sn atoms from Rietveld refinements shown in Table I, the compositions are: $Ba_{7.64}Ga_{16.00}Sn_{29.58}$ for type I and $Ba_{7.37}Ga_{15.69}Sn_{28.63}$ for type VIII.

COMPUTATIONAL METHODS AND DISCUSSION

Ab-initio calculations were carried out using the full-potential linearized augmented plane-wave method as implemented in the WIEN2k code [9], for calculation of the electric field gradients (EFG's), with subsequent numerical simulation of NMR lineshapes. In all cases we used the generalized gradient approximation, with the Perdew-Burke-Ernzerhof formalism for the exchange-correlation electronic term.

We considered 16 different superstructures with distinct occupation of framework sites. These are summarized in Table II, where the first three columns indicate the number of Ga atoms per cell in each site of the parent $Pm\bar{3}n$ structure, and the fourth column shows the number of adjacent Ga-Ga pairs per cell. We retained the cubic cell symmetry, leaving 54 independent atoms ($P1$ space group), except for a few cases allowing higher symmetry. Half of these configurations were taken from previous work on $Ba_8Ga_{16}Ge_{30}$ [10] and $Ba_8Al_xGe_{46-x}$ [11] where the minimum energy configurations where found. Additional configurations were modeled after the proposal by Kozina *et al*. [12] for $Ba_8Ga_{16}Sn_{30}$. In the latter work, EXAFS simulations indicated the number of Ga-Ga bonds to be 15% ± 5% of all framework bonds, corresponding to a range of 3 to 6 Ga-Ga bonds per unit cell. By Rietveld refinements of XRD it was found that the Ga framework occupation is close to 4, 6, 6 in the 6*c*, 16*i* and 24*k* sites, respectively.

All superstructures in our calculations were minimized in volume and structural parameters. The configurations in Table II are arranged from lowest to highest difference formation energy. The formation energy was calculated from the equation $E_f(Ba_8Ga_{16}Sn_{30}) = E_{Ba8Ga16Sn30} - 8E_{Ba} - 16E_{Ga} - 30E_{Sn}$, where E_{Ba} is the energy per Ba atom in Ba metal, similarly for all others. The lowest formation energy was for the configuration 3-1-12-0, where the four numbers correspond to the first four columns in Table II. This configuration also corresponds to

the lowest energy configuration in the case of $Ba_8Ga_{16}Ge_{30}$ [10] and $Ba_8Al_{16}Ge_{30}$ [11]. The absolute 3-1-12-0 formation energy is –17.8122 eV. However, 3-5-8-0 is almost identical in energy, and moreover is in close agreement with the Ga framework occupation obtained through Rietveld refinements. This configuration (with per-site occupation very close to a random configuration) was not considered in previous studies [10,11].

Table II: Ga framework occupation for $Ba_8Ga_{16}Sn_{30}$ with the type-I parent structure. Two different 4-6-6-4 and 4-6-6-3 configurations have been included.

6*c*	16*i*	24*k*	Ga-Ga	ΔE (eV)	6*c*	16*i*	24*k*	Ga-Ga	ΔE (eV)
3	1	12	0	0	5	3	8	4	0.8898
3	5	8	0	0.0159	4	6	6	4	0.9513
3	4	9	0	0.1742	4	6	6	2	1.0774
3	2	11	0	0.2026	4	6	6	0	1.1973
3	3	10	0	0.3295	4	6	6	5	1.3009
3	4	9	2	0.3844	4	6	6	3	1.4388
4	2	10	2	0.4024	4	6	6	1	1.4400
4	6	6	4	0.6855	4	6	6	3	2.2125

From the results reported in Table II it is also clearly seen that Ga-Ga bonds are not energetically favorable, as the formation energy generally increases as the number of Ga-Ga bonds increases, and the lowest-energy configurations found all contain no Ga-Ga bonds. Thus it appears that zero Ga-Ga bonds is most favored, which follows the general trend observed in previous studies [10,11] for Ba-Al-Ge and Ba-Ga-Ge materials.

From the *ab initio* calculations we obtained electric field gradients (EFG's) for each Ga site from the calculated all-electron charge distribution, using a method used in recent years with considerable success for analysis of NMR spectra [13]. This method has been previously applied to $Ba_8Al_xGe_{46-x}$ [11] with excellent results. From computed EFG matrix elements the quadrupole lineshape was simulated by summing a contribution from each m to m+1 transition for $I = 3/2$ ^{71}Ga, with a weighting factor $\sqrt{(I+m)(I-m+1)}$ for each m, and using standard expressions for the angular dependence [14], including the first and second-order quadrupole shift for each transition. The nuclear quadrupole moment used for ^{71}Ga was $Q = 0.11\times10^{-28}$ m^2.

Four different configurations are compared in Figure 1, including the two lowest energy and the 4-6-6-4 and 5-3-8-4 configurations. It is seen that the best fit to the data is represented by the 5-3-8-4 configuration. Along with 5-3-8-4, the proposed [12] 4-6-6-4 and 4-6-6-5 (not shown) are similar but their calculated lineshapes have a larger deviation from the experimental results. Comparing simulations (not shown) for all of the configurations in Table II, none yields an agreement as close as these three. Generally, the width of the simulated satellite spectrum becomes broader as the number of Ga-Ga bonds increases, since the asymmetry induced by Ga-Ga bonds results in a larger EFG. This is shown for the four configurations in Figure 1. Increased EFG's also lead to increased second-order quadrupole broadening of the central line.

In Figure 2 only the simulations for the best fit configurations are shown. For both the agreement is reasonable, although 5-3-8-4 is closest to the NMR results. These configurations indicate a number of Ga-Ga bonds similar to what was previously obtained from EXAFS measurements [12]. Since the NMR resonance width varies rapidly with the number of Ga-Ga bonds, these results point to 4 per cell as the most likely number, even though the calculated energies for these configurations are higher than those of the ground state configuration. It is not

entirely clear why the lowest energy configurations do not appear to be favored as they are in $Ba_8Ga_{16}Ge_{30}$ [10] and $Ba_8Al_{16}Ge_{30}$ [11], although the calculated results (Table II) indicate a generally smaller energy difference between different configurations than, for example, in $Ba_8Al_{16}Ge_{30}$ [11]. Also the results in Table II indicate that the 4-6-6-*x* configurations tolerate Ga-Ga contacts better than other configurations, since among these the 4-6-6-4 configuration has the lowest energy. With more phase space to explore, such a configuration might be favored on the basis of configurational entropy.

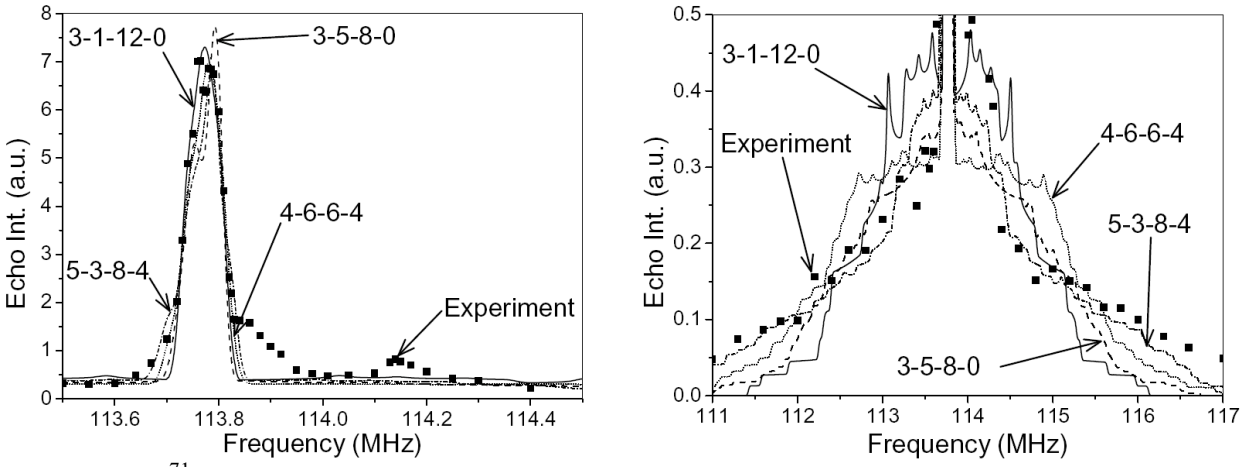

Figure 1: ^{71}Ga NMR lineshape measurements together with 4 calculated configurations: (a) central transition spectral region, (b) satellite region.

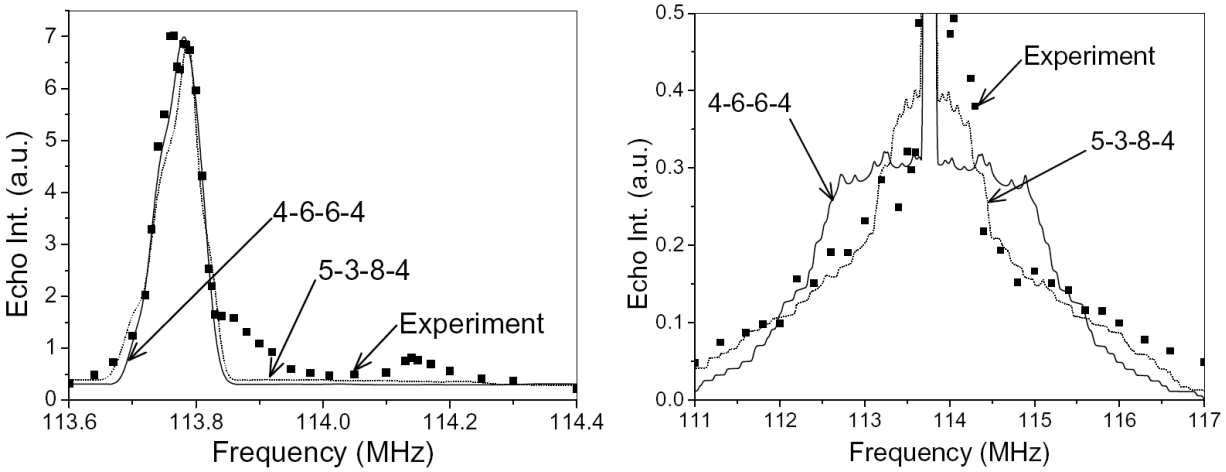

Figure 2: Lineshape measurements together with best fitting configurations (a) central transition, (b) satellites.

For the low-energy minimized type-I configurations, we also find that the Ga-Ga framework bonds are shortened in the calculated results, in general agreement with the trend identified experimentally through EXAFS [12]. Among the structures considered here, we looked carefully at the distribution of bond lengths in the 3-1-12-0, 3-5-8-0, 3-4-9-0, 4-6-6-4, 4-6-6-5, and 5-3-8-4 superstructures, the first three being the most stable calculated structures. In each configuration the average framework bond length falls between 2.77 and 2.79 Å. These

values are 1–2% larger than the experimental average obtained crystallographically [5]; such a difference is typical of DFT calculated results using the PBE-GGA method [15]. The average Sn-Sn bond length is 2.89 Å in the three structures with no Ga-Ga bonds, and it is 2.86 Å in the 4-6-6-4, 4-6-6-5 and 5-3-8-4 configurations. The average Ga-Sn bond length ranges from 2.72–2.76 A, while the Ga-Ga bond average for 4-6-6-4, 4-6-6-5 and 5-3-8-4 is 2.67 Å. Thus the calculated Ga-Ga bonds are reduced by an average of 4% relative to the average framework bond, consistent with the experimental trend, although smaller by almost a factor of two than the reported reduction amount [12].

In our previous study on the $Ba_8Al_{16}Ge_{30}$ system [11], calculated Al-Al bond lengths exceeded those of Ge-Ge by an average of 0.06 Å, a result that we have since observed for a number of additional configurations. An EXAFS report for $Ba_8Ga_{16}Ge_{30}$ [16] also indicated a small lengthening ~0.02 Å of group-III atom bond lengths relative to the framework average, independent of carrier type. Thus the trend in type-I $Ba_8Ga_{16}Sn_{30}$ opposes that of the two Ge-based systems. The latter results may be explained by bond destabilization; indeed, for $Ba_8Al_{16}Ge_{30}$ our calculated results indicate an energy cost per Al-Al bond that is roughly twice the values found here for $Ba_8Ga_{16}Sn_{30}$. On the other hand, in $Ba_8Ga_{16}Sn_{30}$ the relative atomic sizes appear to dominate; the sum of covalent radii for Ga-Ga (2.5 Å) is considerably smaller than the expanded framework bond length in this material.

We also find that the large-cage Ba atoms have significant off-center displacements in the type-I $Ba_8Ga_{16}Sn_{30}$ configurations; for example in 3-1-12-0 the displacement is 0.5 A from the cage center. This displacement is toward the center of a Ga-Sn pair occupying 24*k* sites of the original type I lattice. Such large displacements are consistent with the reported very low-frequency vibrational mode for this cage [5]. However, calculated configurations do not feature large distortions of the cage shape itself.

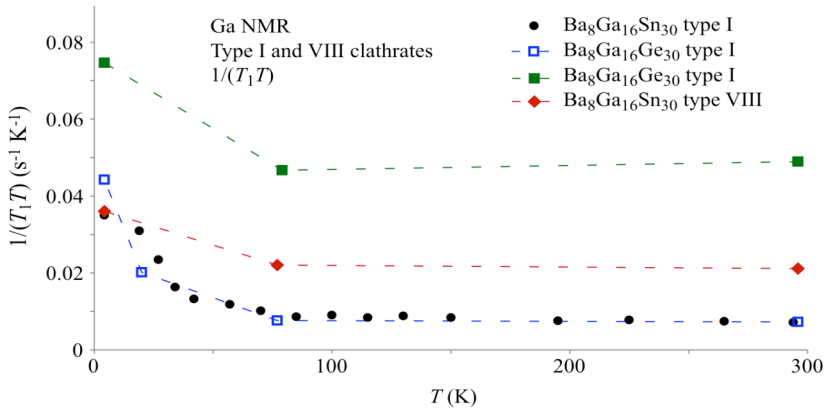

Figure 3: ^{71}Ga NMR T_1T results for samples studied here, compared to results for $Ba_8Ga_{16}Ge_{30}$.

Temperature-dependent results for the ^{71}Ga NMR spin-lattice relaxation time (T_1) are shown in Figure 3, which also includes previous results for two $Ba_8Ga_{16}Ge_{30}$ samples [17]. At higher temperatures the constant $(T_1T)^{-1}$ values indicate Korringa behavior [18], indicating the doping of these materials into the low-density metallic regime, as typically observed in these materials. Preliminary measurements show that the $(T_1T)^{-1}$ enhancement at low T is due to a quadrupole mechanism, and hence due to low-frequency atomic motion.

CONCLUSIONS

We have synthesized type-VIII and type-I $Ba_8Ga_{16}Sn_{30}$ clathrates. NMR lineshape measurements coupled with *ab initio* calculations for type I gave a good fit, with best agreement corresponding to the 5-3-8-4 configuration. The best fit results indicate four Ga-Ga bonds, similar to what was previously extracted from EXAFS simulations. Note that in this case this configuration does not have the lowest energy in our *ab initio* results, and we speculate that the configurational entropy might dominate. The calculated Ga-Ga bond-lengths are the shortest framework bonds, in agreement with reported experimental results, although this trend is opposite to that observed in $Ba_8Ga_{16}Ge_{30}$ and $Ba_8Al_{16}Ge_{30}$. In addition we find a significant displacement of the large-cage Ba atom.

ACKNOWLEDGMENTS

This work was supported by the Robert A. Welch Foundation, Grant No. A-1526, and by the National Science Foundation (DMR-0103455).

REFERENCES

1. G. A. Slack, MRS Symp. Proc. **478**, 47 (1997).
2. H. Kawaji, H. Horie, S. Yamanaka, and M. Ishikawa, Phys. Rev. Lett. **74**, 1427 (1995).
3. R. P. Hermann, V. Keppens, P. Bonville, G. S. Nolas, F. Grandjean, G. J. Long, H. M. Christen, B. C. Chakoumakos, B. C. Sales, and D. Mandrus, Phys. Rev. Lett. **97**, 017401, (2006).
4. K. Suekuni, M. A. Avila, K. Umeo, H. Fukuoka, S. Yamanaka, T. Nakagawa, and T. Takabatake, Phys. Rev. B **77**, 235119, (2009).
5. M. A. Avila, K. Suekuni, K. Umeo, H. Fukuoka, S. Yamanaka, and T. Takabatake, Appl. Phys. Lett. **92**, 041901, (2008).
6. D. Huo, T. Sakata, T. Sasakawa, M. A. Avila, M. Tsubota, F. Iga, H. Fukuoka, S. Yamanaka, S. Aoyagi, and T. Takabatake Phys. Rev. B **71**, 075113 (2005).
7. B. H. Toby, J. Appl. Cryst. **34**, 210 (2001).
8. C. S. Lue and J. H. Ross, Jr., Phys. Rev. B **58**, 9763, (1998).
9. P. Blaha, K. Schwarz, G. Madsen, D. Kvaniscka, and J. Luitz, *Wien2k An Augmented Plane Wave+Local Orbitals Program for Calculating Crystal Properties* (Technische Universitat Wien, Austria, 2001).
10. N. P. Blake, D. Bryan, S. Latturner, L. Mollnitz, G. D. Stucky, and H. Metiu, J. Chem. Phys. **114**, 10063 (2001).
11. W. Gou, S. Y. Rodriguez, Y. Li, and J. H. Ross. Jr., Phys. Rev. B **80**, 144108 (2009).
12. M. Kozina, F. Bridges, Y. Jiang, M. A. Avila, K. Suekuni, and T. Takabatake, Phys. Rev. B, **80**, 212101, (2009).
13. T. J. Bastow and G. W. West, J. Phys.: Condens. Matter **15**, 8389, (2003).
14. G. C. Carter, L. H. Bennett, and D. J. Kahan, *Metallic Shifts in NMR,* Pergamon, New York, (1977).
15. J. P. Perdew, K. Burke, and M. Ernzerhof, Phys. Rev. Lett. **77**, 3865 (1996).
16. Y. Jiang, F. Bridges, M. A. Avila, T. Takabatake, J. Guzman, G. Kurczveil, Phys. Rev. B **78**, 014111 (2008).
17. W. Gou, Ph.D. Dissertation, 2007 (unpublished).
18. C. P. Slichter, *Principles of Magnetic Resonance,* New York: Springer-Verlag, (1990).